Scripta Materialia 144 (2018) 56–59

Contents lists available at ScienceDirect

Scripta Materialia

journal homepage: www.elsevier.com/locate/scriptamat

Regular Article

Silicon activation volumes for fracture as affected by hydrogen

Claire S. Teresi *, William W. Gerberich

University of Minnesota, 421 Washington Ave SE, Minneapolis, MN 55455, USA

ARTICLE INFO

Article history:
Received 21 August 2017
Received in revised form 20 September 2017
Accepted 20 September 2017
Available online 1 October 2017

Keywords:
Fracture
Hydrogen embrittlement
Nanoindentation

ABSTRACT

Silicon is widely used at the small scale in environments where possible hydrogen can be introduced to the material. In this work, small scale mechanical testing with nanoindentation coupled with thermal gas hydrogen charging are used to determine activation volumes and fracture toughness in material with and without hydrogen charging. Hydrogen is found to increase microcracking in micropillars at the sub-micron scale. Additionally, it lowers and produces a large size dependence in fracture toughness not observed in single-crystal silicon material without hydrogen charging.

Silicon is increasingly being utilized in MicroElectroMechanical Systems (MEMS), particularly for components at the micron to nanometer length scale where the increased surface-to-volume ratio of the material can impact physical properties. For this reason, it is imperative to improve and expand the understanding of mechanical behavior of Si at length scales appropriate for MEMS. Si is generally considered a brittle material; however, for small length scale components, plastic deformation and cracking can occur and must be accounted for in component design [1,2]. At small Si volumes, this can be impacted by dopants as well as the addition of hydrogen [3]. Since MEMS devices are often produced in acidic environments, there are opportunities for hydrogen to diffuse into the material. Observations of humidity producing MEMS operational issues in harsh environments have been previously reported [4,5] as well as hydrogen embrittlement effects on microelectronic properties [6]. Additionally, this may demonstrate a path to resolve long standing issues of what hydrogen concentrations in what materials require more in-depth solutions involving hydrogen enhanced decohesion (HEDE) [7] or hydrogen enhanced localized plasticity (HELP) [8]. This work focuses on plastic deformation and fracture by attempting to determine or estimate the activation volume for dislocation initiation or motion in both the as-received and hydrogen charged material.

Polished phosphorus-doped (100) Si wafers ($\rho = 1$–$10\ \Omega$) were used for this work as such n-type dopants have been found to produce an increase in the dislocation velocity in silicon [9]. Wafers were used for nanoindentation testing, and uniaxial compression tests were completed on micropillars created using a FEI 200 3D Quanta focused ion beam. All material used in this work was treated with an HF-HCl solution post FIB-processing to mitigate oxide effects and Ga damage [10]. To determine pillar dimensions for stress and strain calculations, pillar imaging was completed before and after testing with a JEOL 6700 SEM at 5 keV. In addition, SiO_2 thickness was measured before and after hydrogen charging with a VASE ellipsometer.

Material was thermally hydrogen charged at Sandia National Laboratory at 573 K and 140 MPa H_2 for 10 days. In attempts to limit hydrogen outgassing until testing, hydrogen charged samples were kept in dry ice. Then, samples were warmed to room temperature and tested with a Hysitron TI-900 Triboindenter with a Berkovich tip for nanoindentation and a 5 μm radius conical tip for pillar compression. To determine activation volumes for each loading condition, all testing included multiple strain rate jumps where strain rate was changed by approximately an order of magnitude. Specifically, micropillar compression directly compared changes in strain rate to changes in stress [11], while nanoindentation testing compared strain rate changes to relative hardness values [12]. As discussed later, activation volumes from the hydrogenated pillar data could not be used. Nanoindentation was controlled by maintaining a constant effective strain rate of $2\dot{\varepsilon} = \dot{P}/P$ [13,14]. Apparent activation volume calculations were attempted in both testing conditions through [11,12,15]:

$$V^*_{nanoindentation} = \sqrt{3} k_B T \left(\frac{\partial \ln \dot{\varepsilon}}{\partial \sigma^*} \right)_T \tag{1}$$

and

$$V^*_{micropillar} = \frac{k_B T}{\left(\partial \tau^* / \partial \dot{\varepsilon}\right)_T}. \tag{2}$$

Here, T is temperature, $\dot{\varepsilon}$ is strain rate, τ^* is the effective shear stress, and σ^* is the effective normal stress. For indentation, it is assumed that

* Corresponding author.
E-mail address: teres007@umn.edu (C.S. Teresi).

https://doi.org/10.1016/j.scriptamat.2017.09.035
1359-6462/

the equivalent compressive stress is related to the hardness by dividing by an empirical constant of 2.4 [16–19]. Dislocations in silicon can operate by partial (b = 0.222 nm) or full dislocations (b = 0.38 nm) [1]; partial dislocations were assumed for the calculations for both micropillar compression and nanoindentation. The behavior of Si under load is relatively well studied and dislocation behavior is summarized as functioning on the {111} planes in a shuffle or glide set, but the shuffle set is thought to and has been observed to operate at room temperature and high stresses [20–22] as in these tests.

Hardness and modulus values from non-hydrogen charged nanoindentation matched well with excepted values for (100) Si [23,24] at 10.3 ± 0.3 GPa and 131 ± 2 GPa, respectively. To observe potential size effects with micropillar testing, three pillar diameters were tested; mean and standard deviation values for shear stress decreased with increasing size as shown in Table 2. While some pillars exhibited brittle failure upon testing, the majority exhibited some plastic deformation, see Figs. 1(a) and 2. The apparent strain increases seen in Fig. 1(a) with hydrogen charging are artificially increased due to microcracking at the top of the pillar where a sliding contact developed.

In terms of hydrogen content during testing, there should be some free hydrogen remaining in the silicon material for at least several hours at room temperature, and differences in hardness and modulus values were found up to 24 h after the samples were left at room temperature. The hydrogen charged silicon wafers had modulus and hardness values of 148 ± 3 GPa and 10.7 ± 0.4 GPa respectively. Oxide thickness on a FIB-prepared wafer without hydrogen charging was 2.38 ± 0.4 nm and increased approximately 0.5 nm with hydrogen charging, which does not account for the mechanical property changes observed.

Micropillar samples also demonstrate a time dependence in mechanical behavior – see Fig. 2 for example images of micropillars before and after compression testing. While hydrogen charging seemed to impact mechanical properties significantly, there was no observable difference in the micropillar appearance after hydrogen charging before testing as seen in Fig. 2(b). The first two compression tests on micropillars charged with hydrogen showed extraordinary indications of slip and fracture as large load drops repeatedly occurred at relatively high strains, up to 16%, see Fig. 1(a). While this extreme load-dropping behavior was not apparent in testing after 1 h, pillars still behaved differently than non-charged pillars. Average apparent yield stress for the hydrogen charged micropillars were an artifact of the micropillar nanocracking at the top contact surface. The initial testing results indicate that plastic deformation and/or nanocrack formation becomes easier with the addition of hydrogen in uniaxial compression, but does not appreciably change in nanoindentation. The potential explanations for this behavior are that hydrogen creates defect sites at the Si/SiO_2 interface as previously shown [25,26] and additional tensile residual stresses from hydrogen charging produced increased cracking relative to non-hydrogen charged materials. This is clearly seen in the micrographs of Fig. 2(a) and (c). The results from eccentric micropillar compression tests where slight misalignment of the tip load with the pillar center led to fracture at the pillar base, also support this explanation as shown in Fig. 2(d–e). The fractography analysis of the remaining material at the base resulted in an obvious critical crack length that resulted in pillar failure. Assuming that K_{IC} is constant for a given pillar size and the crack opening is very small relative to the pillar length, the stress intensity factor at a crack tip in a square beam is modeled as [27]:

$$K_{IC} = \sqrt{\frac{\pi\alpha}{D}}\left[\frac{6Pe}{D}F_M - PF_N\right]. \quad (3)$$

Here D is the relevant thickness dimension, i.e. the pillar diameter, α is the ratio of critical crack length to diameter, P is the modified applied load, e is the eccentricity factor or the length the load is applied relative to the pillar center, and F_M and F_N are functions of the eccentric and normal force respectively, both dependent on α and are found in [27]. Also, note that e is a relative unknown due to the ex-situ nature of testing. However, considering the size of the indenter tip and pillar, it is estimated that e is relatively small compared to pillar diameter. Here it is assumed to be a constant value of 50 nm for all pillar sizes. The K_{IC} for non-H specimens was found to be 1.5 ± 0.6 $MPa*m^{1/2}$, though some dependence on pillar diameter was noted with smaller pillars having slightly higher average fracture toughness values. In the H-charged specimens, a large dependence of K_{IC} on pillar diameter with slightly less scatter in the data was found. It should be noted that K_{IC} values range from 0.66 ± 0.26 $MPa*m^{1/2}$ for 1 μm diameter pillars to 0.11 ± 0.06 $MPa*m^{1/2}$ for 500 nm diameter pillars, all of which are much smaller than the expected values for silicon. All data are shown in Fig. 3a, and the large standard deviation with these pillars is expected as geometry of the pillar and eccentricity are likely to vary. This evidence supports an embrittlement of Si by hydrogen, and is consistent to the observed effect of hydrogen exacerbating the fracture at $Si\text{-}SiO_2$ interfaces providing increased microcracking at the micropillar contacts [28].

Activation volume calculations, normalized by the Burgers vector cubed, were also attempted for nanoindentation and micropillar compression testing. Nanoindentation results were necessarily revised due to both an increase in flow stress and activation volume with hydrogen charging. These results did not account for the pressure effects from hydrogen charging that are more difficult to predict with the stress state for nanoindentation, but are shown in Fig. 1(b). In the micropillar case, while activation volumes were relatively simple to determine with non-hydrogen charged samples, after hydrogen charging, it was not possible to differentiate stress changes due to strain rate jumps from the discontinuities produced by crack formation and growth. Previously, it was shown that nanotwinning occurs in 40 nm cubes under compression [22]. This involved partial dislocations, giving b^3 to be

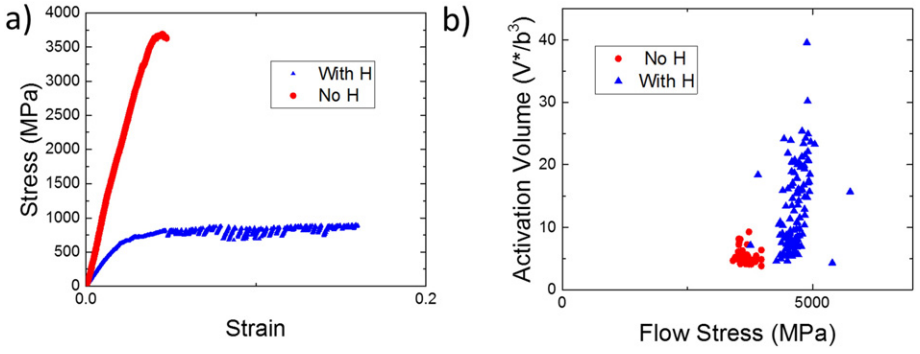

Fig. 1. a) Compression tests for 500 nm diameter Si micropillars without hydrogen charging and immediately after removal from cold storage after hydrogen charging showing likely microcracking by significant load drops. Both micropillars fractured at last point on graph.